

Humidity Sensing Properties of Ferroelectric Compound $\text{Ba}_{0.7}\text{Sr}_{0.3}\text{TiO}_3$ Thin Films Grown by Pulsed Laser Deposition

Hamed A. Gatea^{1,*}, Iqbal S. Naji² and Ameer F. Abulameer²

¹Department of Optics, Faculty of Health and Medical Techniques, Al Ayen University, Thi Qar-Iraq.

²Department of physics, College of Science, University of Baghdad, Baghdad- Iraq.

Received: 21 Feb. 2020, Revised: 22 Mar. 2020, Accepted: 24 Mar. 2020.

Published online: 1 May 2020.

Abstract: BaSrTiO_3 (BST) is a solid solution prepared by Sol-Gel method. A ternary compound of BST is composed of from solid solution BaTiO_3 and SrTiO_3 . BST thin films prepared by PLD method and their humidity sensing characteristics have been investigated. The films were formed on Si substrates with Au electrodes. XRD pattern showed tetragonal phase and no significant change between film and bulk. SEM revealed a uniform distribution of cubic particles shape and nanoparticles size. Capacitive and Resistive humidity sensors were made based on BST/Si thin film used coplaner form and the corresponding sensing properties were investigated. Experimental results showed on that the sensor exhibited high sensitivity and good stability. The humidity relative increased then the capacitive increased and resistivity decreased.

Keywords: BST; humidity relative; capacitive hysteresis; resistivity hysteresis.

1 Introduction

Humidity sensors had various application in environmental control, industrial processing and human comfort [1]. Other applications such as intelligent control of laundry, cooking control for microwave and intelligent of the living environment.

Because of the low cost of electrical circuits, there is a strong tendency towards the use of automatic control, which leads to ceramic oxide generally have been used for the importance of controlling the environment [2]. The types of relative humidity (RH) sensors are based on ceramics, polymer materials and semiconductors.

So far, there are no specific or appropriate materials that meet the requirements of the relative humidity sensors such as high sensitivity, good chemical and thermal stability polymers and humidity sensors [3].

Barium strontium titanate compounds have a perovskite structure that depends on formula ABO_3 where A and B are cation and anion, respectively. The main feature of this structure, when A other ions substitute, it will be maintained perovskite structure [4]. Barium strontium is a

solid solution prepared in this work using sol-gel method, BST compound has been valuable in the last 10 year because it has high dielectric constant and low dissipation factor [5].

Humidity sensors based on water-phase protonic ceramic materials are used in industrial research laboratories [6].

The principle of humidity sensors operation depends on the adsorbed water condenses on the surface of the substance [7]. The conductivity increases when humidity and dielectric constant increase [8]. The mechanism of protonic conduction inside the adsorbed water layers on the surface of the sensing materials was discovered in TiO_2 .

As shown in Fig. (1) Water molecule is adsorbed on-site (a), and adsorption complex form on site (b), which subsequently transfers to surface hydroxyl groups (c). Another water molecule is adsorbed through hydrogen bonds on the two neighbouring hydroxyl groups as shown in (d).

The two hydrogen bonds on water molecule are restricted and cannot move freely. The first physically adsorbed layer is immobile and no hydrogen bonds are formed

*Corresponding author E-mail: hamedalwan14@gmail.com

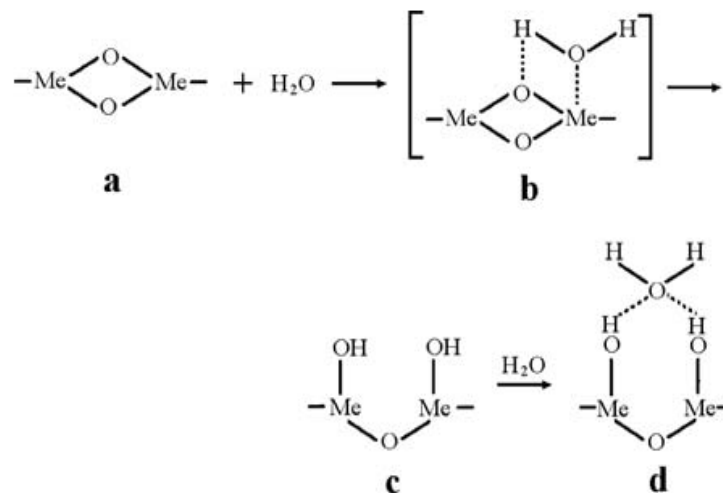


Fig.1: Molecule water sites.

between the water molecules in this layer [9]. The relative humidity (RH), which is the ratio of the actual vapour pressure of water to the saturated vapour pressure at a particular temperature, is commonly used to measure humidity.

Humidity measurement of the ceramic sensor relies electrical properties (conduction and capacitance) due to affect the pores of the active sensor materials which turn on occur by water chemisorption and/ or capillary conduction. Perovskite materials such as BST are protonic ionic conductors which have been used for sensing humidity [10].

2 Experimental Details

Ba_{0.7}Sr_{0.3}TiO₃ ferroelectric was prepared conventional by Sol-Gel method. The starting raw materials were high purity Barium acetate (BDH chemical England, 99.95%), Strontium acetate (Aldrich company, 99.9%), Ti(IV)isopropoxide (97% Aldrich) as the source of barium, strontium and titanate, respectively. Acetic acid (Merck 99.8%) was used as the solvent and 2-methoxy ethanol was used as a stabilizer for Ti(IV) isopropoxide.

The solution refluxed at 110°C for 2 h (till obtained transparent solution slightly tuned to yellow). 2-methoxy ethanol (2-4 ml) was added as a stabilizer that maintains crystal structure for Ti-isopropoxide at room temperature.

Finally, the solutions were dried at 200°C for 2 h to separate water completely with different compositions. The powders were calcined at 700 C for 2h. The powders were ground in a mortar to obtain a fine powder. BST nanoparticles with fine powders, compacted in a cylindrical steel model had (120 mm) internal diameter.

The process was used to press the powder into a pellet

shape to reduce vacancies and porosity between the particles and shrink the size by packing the particles to each other with the average dimension of (120mm) diameter and (2.5-3.0mm) in thickness under (250-300 Mpa).

The pellet was used as the target in the system of pulsed laser deposition, the distance between target and the substrate (2.5 cm) to deposit film on co-planer from with gold electrode.

The morphological and composition properties of the sintered pellets were performed using field emission scanning electron microscopy (FE-SEM) supplemented with energy dispersive spectroscopy model (Hitachi 4700 field emission microscope). The microstructure of all compounds was recorded at room temperature using X-ray powder diffractometer with CuK α ($\lambda = 1.5418 \text{ \AA}$, 30 kV, 30 mA) model (Bruker, Germany) in a wide range of $2\theta = 20^\circ$ - 80° at scanning rate 1 min⁻¹. (100-200 nm).

3 Results and Discussion

Figure (2) indicates the polycrystalline structure of ferroelectric Ba_{0.7}Sr_{0.3}TiO₃. The X-ray diffraction patterns of Ba_{0.7}Sr_{0.3}TiO₃ sintered at different temperature. The XRD pattern of Ba_{0.7}Sr_{0.3}TiO₃ phase has various peaks related to the tetragonal perovskite phase along the (100), (101), (111), (200), (201), (211), (202), (221), (301) planes. The peak positions matched the PDF card no. (00-044-0093). This phase exhibited the P4mm space group with ($a=3.9771 \text{ \AA}$ and $c=3.9883 \text{ \AA}$).

Furthermore, ferroelectric Ba_{0.7}Sr_{0.3}TiO₃ sintered at 1100 °C are BST phase with perovskite structure. There exists no evidence of any additional phase, suggesting that Sr²⁺ ions have entered the unit cell maintaining the perovskite structure of the solid solution.

The ferroelectric Ba_{0.7}Sr_{0.3}TiO₃ sintered at 900, 1000 °C.

There exist two weak diffraction peaks as a secondary phase (+, +) besides the peaks of BST phase, which appeared at ($2\theta=24.21, 26.8^{\circ}$) and (28.8°) belong to intermediate oxycarbonates such as $Ba_2Ti_2O_5CO_3$, and $(Ba,Sr) Ti_2O_5CO_3$. The most probable crystalline impurity is Sr_2TiO_4 , $SrTiO_4$, $Sr_3 Ti_2O_7$ almost appear at 44.6° . The major peaks shifted towards 2θ angles when

Sr^{+} ions increase. This happened due to the decreased interatomic spacing of the BST which affected by the radius of Sr^{+} ion (1.13 \AA) which is smaller than Ba^{+} ions (1.35 \AA).

Fig. (3), shows XRD pattern for $Ba_{0.7}Sr_{0.3}TiO_3$ film. No significant occurs between film and bulk material that belongs to complete crystalline for samples film or bulk.

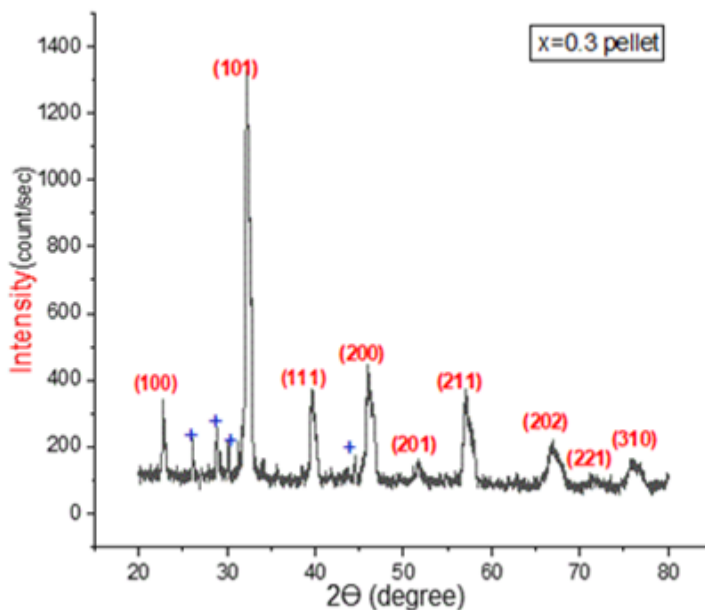


Fig. 2: XRD patterns of $Ba_{0.7}Sr_{0.3}TiO_3$ powders.

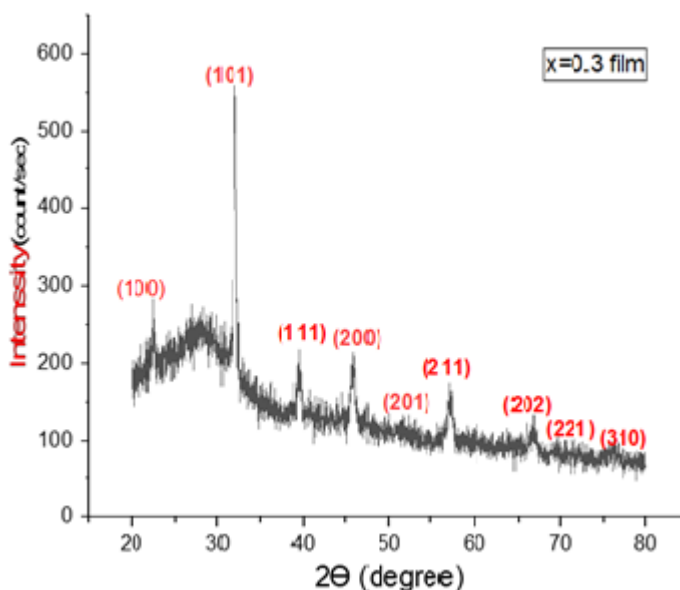


Fig. 3: XRD patterns of $Ba_{0.7}Sr_{0.3}TiO_3$ film.

According to Fig (4) calculated grain size of $Ba_{0.7}Sr_{0.3}TiO_3$ sintered at 900, 1000 and 1100 °C is 73.38, 193.378 and 278.45 nm, respectively, using ImageJ program (1.51j8) which reveals that the grain size increases with the rise of sintering temperature.

It shows SEM micrograph of $Ba_{0.7}Sr_{0.3}TiO_3$ sintered at various sintering temperature. In addition,

sintering temperature has an obvious effect on the grain size indicating that the grain size increases with the rise of sintering temperature.

Fig (5), exhibits that images for SEM with different scale and the particles size are defined by software ImageJ (34-42 nm). Also, thickness of film calculated by cross-section technique approximately (93-134 nm).

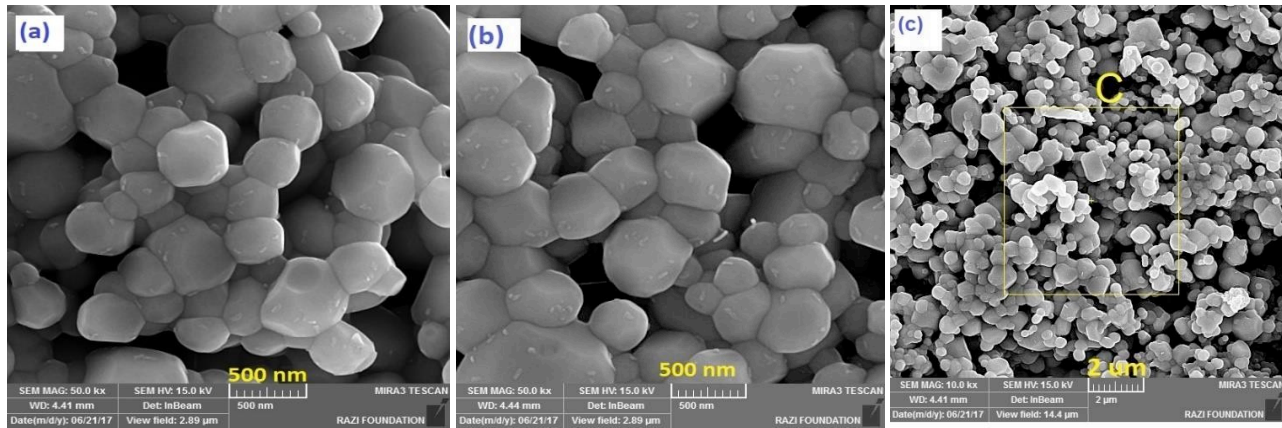


Fig. 4: FESEM images for $Ba_{0.7}Sr_{0.3}TiO_3$ pellets sintering at 1000 °C.

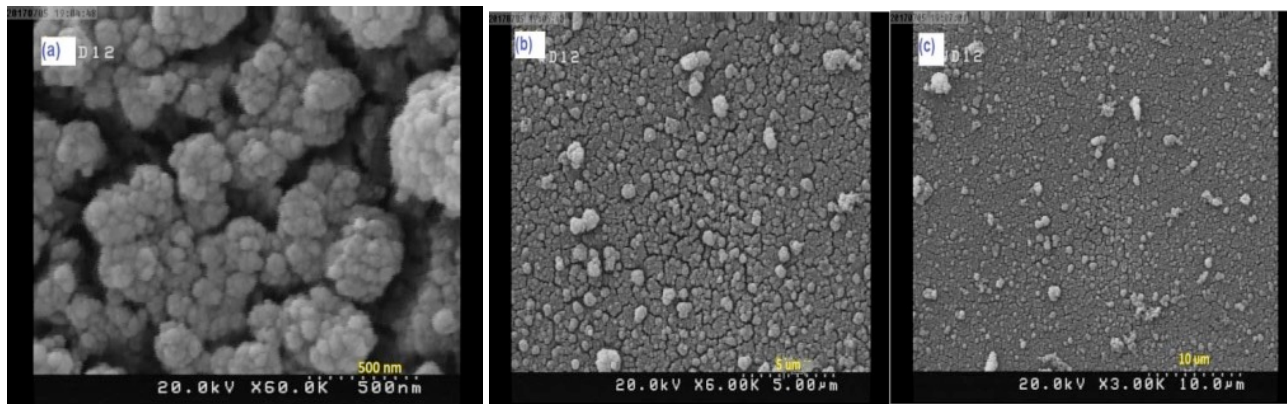


Fig. 5: SEM images for $Ba_{0.7}Sr_{0.3}TiO_3$ films deposited on Si substrate annealing at 700 °C.

3.1 Sensor Device Measurements Analysis

These results manifest the investigation of BST compounds as active materials in capacitive - resistive surface type multifunctional sensors. Thin films of BST deposited by PLD method. The mode of operation for the capacitive type sensors is a change in the dielectric constant of the humidity sensing layer with varying humidity levels. However, a resistive humidity sensor works on the resistance-variation principle. The BST thin film surface-type humidity sensors of different frequencies (1 kHz, 20 kHz, 50 kHz and 100 kHz) are undertaken and the effect of humidity on the capacitance and resistance is examined.

Humidity on the capacitance and resistance is examined. The electrical properties of BST compounds change because of water-adsorption processes on their surface, so they are used as humidity sensors. The detection mechanism of ionic -type humidity sensor is strictly related to the aforementioned water-adsorption mechanisms.

The measuring humidity-sensitive variations in conductivity can detect moisture, which ionic type oxide undergoes because of water adsorption. Resistivity decreased exponentially with humidity.

Surface-related effects. A different value of The conduction mechanism based on the surface coverage of adsorbed water. The relative humidity of barium strontium titanate oxide is related to water molecule adsorption sites,

and they are greatly influenced by the presence of oxygen atoms x leads to a different structure, density and rough surface which in turn to a variety of pores. The different microstructure was obtained using BST powders having different grain size, surface area and porosity, especially those prepared by and lattice defects at the oxide surface.

The control of porosity and surface activity is of primary concern for ionic type humidity sensors because they rely on Sol-Gel.

3.2 Capacitive Humidity Sensor

Fig. (6) Shows the capacitive humidity sensing properties of the BST/Si sensor under different frequencies at R.T. The capacitance of BST/Si sensor increased with increasing relative humidity RH. That behaviour is attributed to the effect of multilayers of physically adsorbed water. The adsorbed water molecules increase when increasing RH. As known, the capacitance was strongly dependent on the measuring frequency. The behaviour shows capacitance decrease with increasing frequencies that belong to the increased difficulty for dipoles of water molecules to re-orient with increasing frequency. The value of capacitance depends on the polarizability of the materials. Mechanism polarization involves devires source including electronic, ionic, dipolar and space charge. In this case in the humidity sensor, the dipolar polarization is present due to dipoles (H_2O) absorbed by thin BST films. The electronic polarization also is most universal and arises due to relative displacement of the orbital electrons.

3.3 Resistive Humidity Sensor

Fig. (7) Shows the relation between resistance and

RH of BST thin film deposited by PLD method on Si substrate at R.T. The great influence of the humidity sensitivity on the resistance.

The best results were shown by sample $x=0.3$. The relative humidity (RH) dependence of impedance of films measured at $35\text{ }^{\circ}\text{C}$ for various frequencies is shown in Fig. (7). That shows the resistive of films decreases with increasing relative humidity and RH depends on the frequencies of the applied electric field. There are several reasons for the enhancement in conductivity of BST thin film with the elevation of relative humidity level. First, the increased conductivity of the BST film due to both ionic and electronic conduction the absorption of water enhances the ionic conductivity of BST thin film due to the increased dielectric constant. Second, may the disassociation of water molecules into ions may occur, resulting in the increase in conductivity of the thin film.

The frequency dependence of resistive – humidity sensor and the sensitivity of the resistive decreased with the increase of the frequency.

The capacitance-humidity sensor covers the broad range rather than resistive-humidity sensor. To cover the whole range, it must use the impedance- humidity sensor because the impedance (z) correlates between capacitance and resistance when measured in parallel Fig. (8) exhibits decreased capacitance and resistance with increased frequencies. This occurs because when increase frequencies, some of the mechanisms of polarization disappear as mentioned above.

Similarity, the resistance reduced when frequencies increased due to decreased dielectric constant. Thus, conductivity decreased.

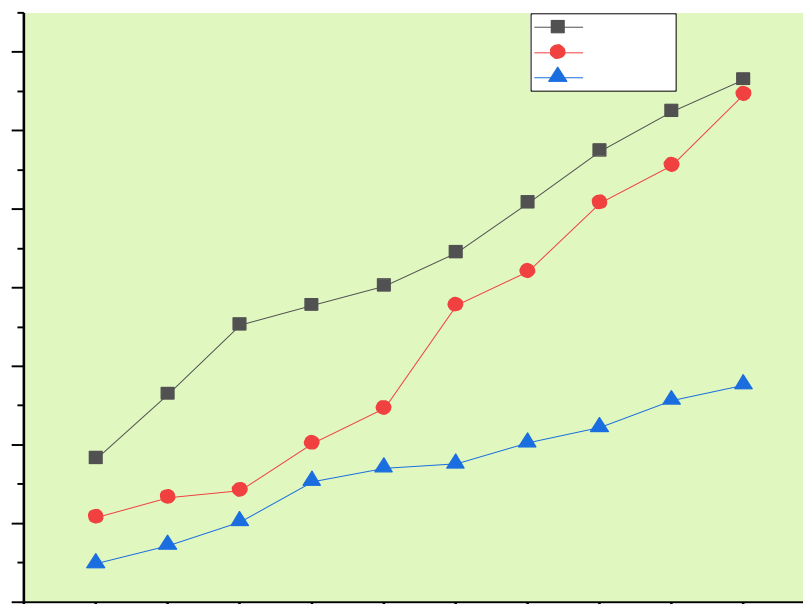


Fig.6: The variation capacitance vs relative humidity sensor (a) $x=0.3$.

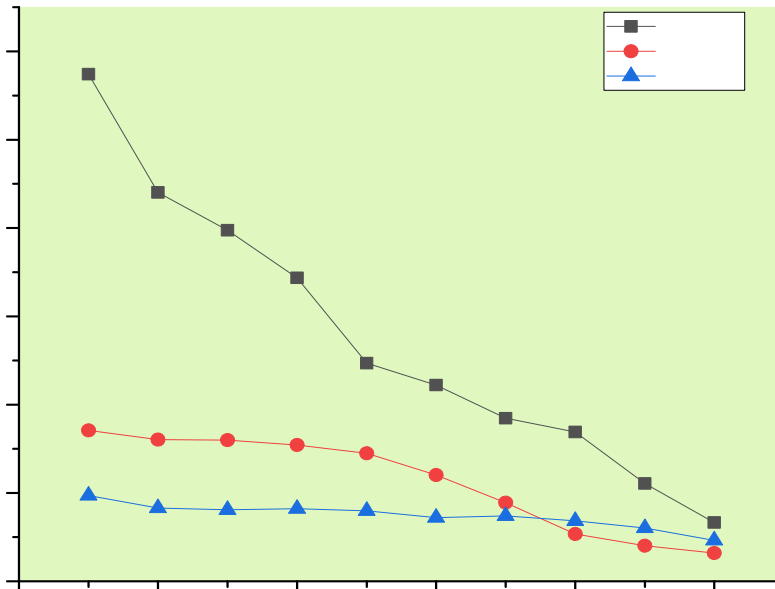


Fig. 7: The variation Resistance vs RH% with a different frequency of samples (b) $x=0.3$.

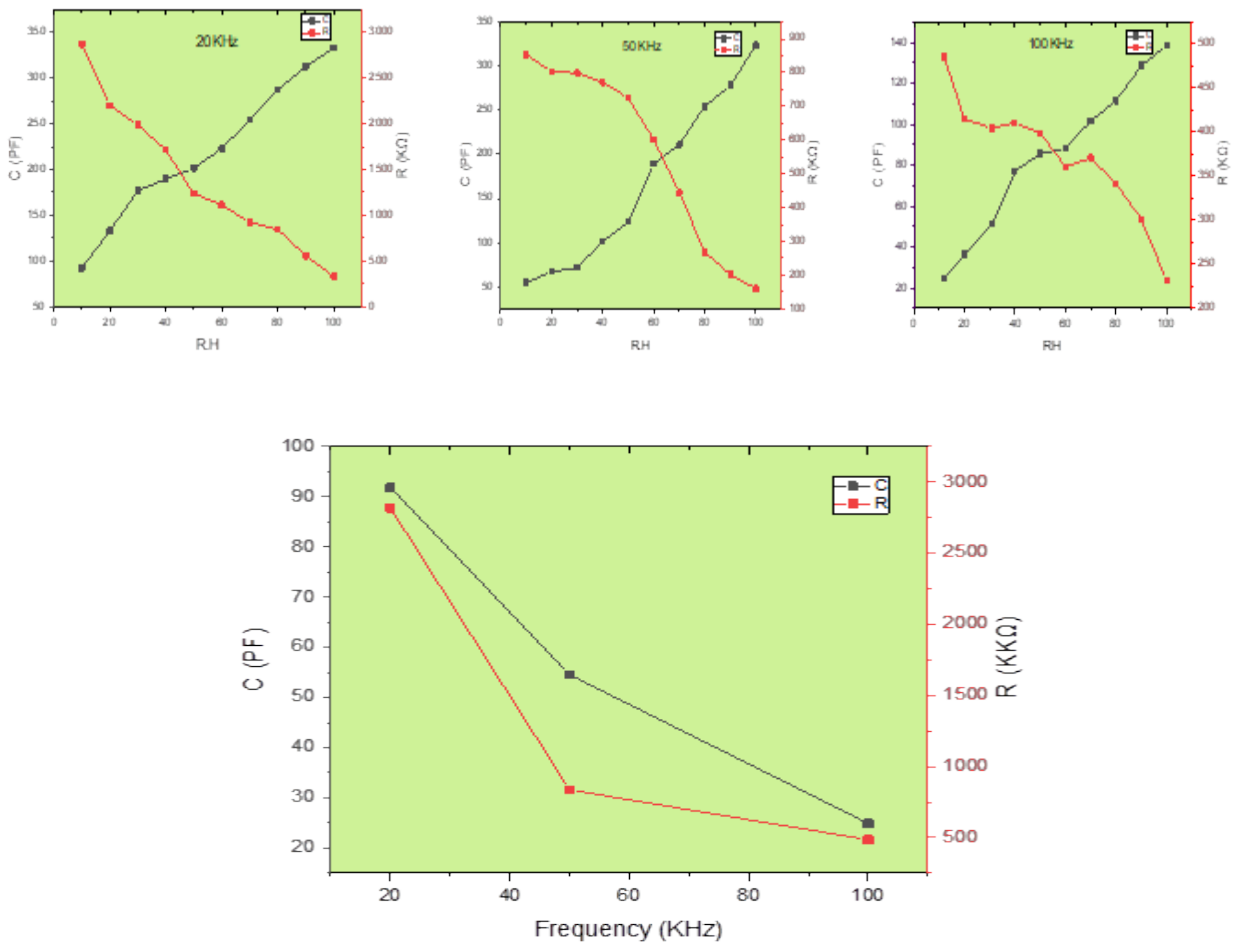


Fig.8: Variation Capacity and Resistance vs RH% with different frequencies Frequency (kHz).

Humidity sensors based on the principle of absorption are hysteresis. Hysteresis is the tendency of measuring devices that do not return, completely to their original state after a change is measured. This occurs due to the formation of clusters of absorbed water in the active thin film. i.e when measuring relative humidity, it can be a main source of error and common problem in humidity sensors based on absorption and desorption. The size and geometry of the pores are related to their slow diffusion time. The large pore

size reduces the response time but and the sensitivity properties so it is difficult to make fast and sensitive humidity sensor. Besid on Fig. (9), it has been determined that the sensor has acceptable values of hysteresis. Capacitive measurements have a hysteresis of 11-15%. The sensor should follow the same capacitance paths when it is cycled back from high to low RH. Moreover, it shows resistive humidity sensor hysteresis, the resistive values have a hysteresis of 10-16%.

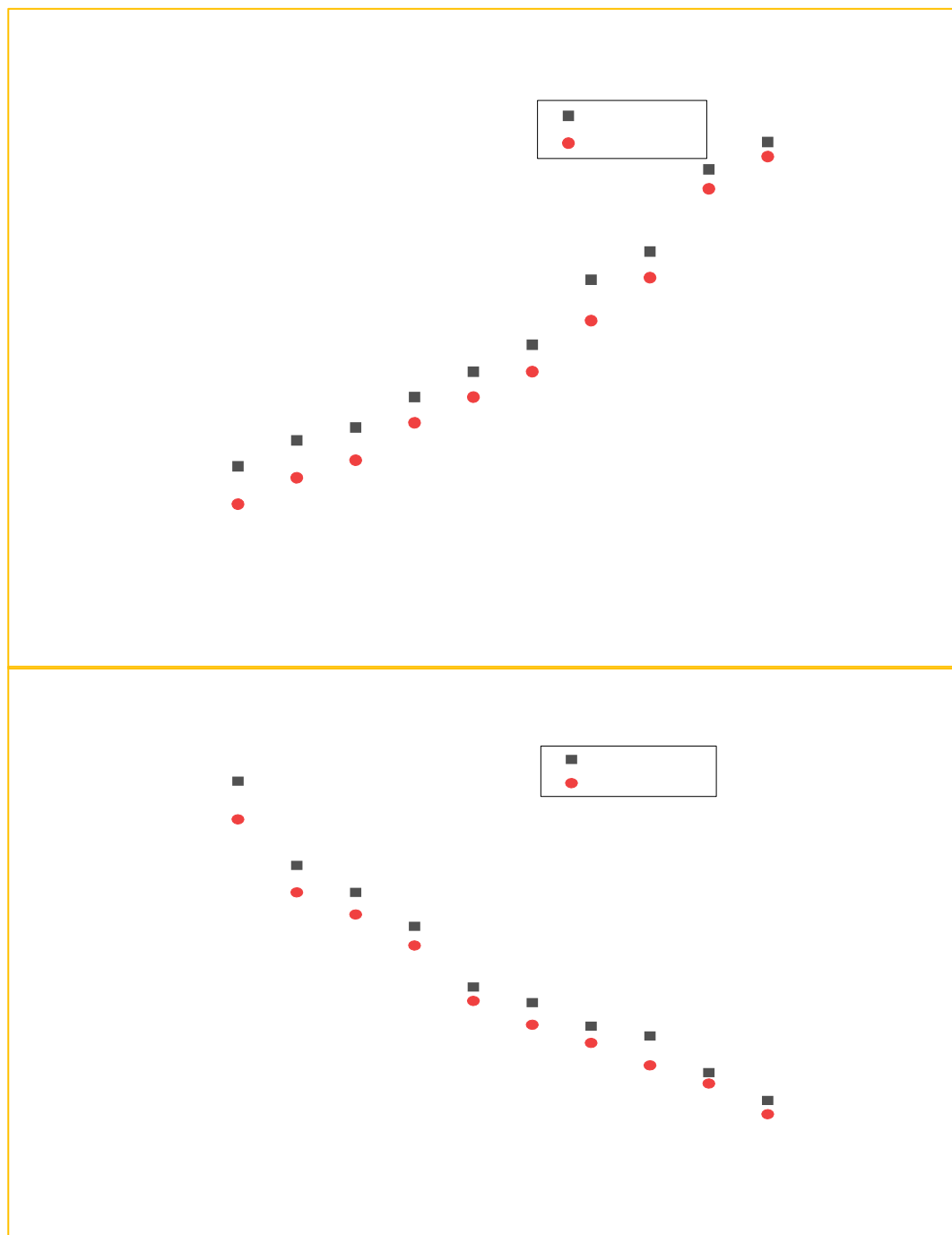


Fig. 9: Hysteresis of Au/BS/Au films capacitance humidity sensor for $x=0.3$.

4 Conclusions

Barium strontium titanate (BST) thin film made by pulsed laser deposition technique are very sensitive to relative humidity (RH). BST thin film fabricated as coplaner form with gold electrode deposited by thermal evaporation technique. BST film is oxide metal with formula ABO_3 that has perovskite structure. XRD pattern shows tetragonal phase for ferroelectric compound $Ba_{0.7}Sr_{0.2}TiO_3$. SEM defines the particles size for different samples with different sintering temperature (1000, 1100 C), when increasing sintering temperature increase particles size and which in turn change in electric properties of samples.

The films of $Ba_{0.7}Sr_{0.3}TiO_3$ were deposited onto silicon substrate using the PLD controlled in the region of several hundred nm as estimated using cross-section technique. The film's response of the obtained sensors was measured upon varying relative humidity from 10% to 100%.

The change in capacitance of BST film with humidity demonstrated that this film can be used as a humidity sensor. Good humidity sensitivity could be attributed to the combined effects of physisorption and chemisorption. The capacitance increased with increased humidity and the resistance decreased with increasing humidity sensor.

Availability of Data Material: Data will not be shared because they can promote designing a better photonic sensor with high-quality factor and sensitivity.

Funding: No funding support this work.

Acknowledgment: I will thank all person contribution, support and encouragement in carry out this work.

References

- [1] Simion C. E., Sackmann, A., Teodorescu, V. S., Rus, C. F., and St, A., Chemical Room temperature ammonia sensing with barium strontium titanate under humid air background, *Sensors Actuators B Chem.*, **220**, 1241–1246 (2015).
- [2] Hua, S. X., Hai jun xu, jin Hu, Wei Fen, Xin jian Li, Structure and humidity Sensing properties of barium strontium titanate / silicon nanoporous pillar array composite films, *Thin Solid Films.*, **517(2)**, 929–932 (2008).
- [3] Andrii Buvailo, Yangjun Xing, Jacqueline Hines, Eric Borguet, Thin polymer film based rapid surface acoustic wave humidity sensors, *Sensor and Actuators B.*, **156**, 444–449 (2011).
- [4] N. Ichinose, Electric ceramics for sensor, *Am .Ceram.Soc. Bull.*, **64**, 1581–1585 (1985).
- [5] Singh, M., Yadav, B. C., Ranjan, A., Kaur, M., and Gupta, S. K., Chemical Synthesis and characterization of perovskite barium titanate thin film and its application as LPG sensor, *Sensors Actuators B.Chem.*, **241**, 1170–1178,

(2017).

- [6] Zhi Chen and Chi Lu, Humidity Sensors: A Review of Materials and Mechanisms, *Sens. Lett.*, **3**, 274–295 (2005).
- [7] Agarwal, S. and Sharma, G. L., Humidity sensing properties of (Ba, Sr) TiO_3 thin films grown by hydrothermal-electrochemical method, *Sensors Actuators B.*, **85**, 205–211 (2002).
- [8] Bernard M. Kulwicki, Humidity Sensors, *J. Am. Ceram. Soc.*, **74(4)**, 697–708 (1991).
- [9] P.M. FAIA, C.S. Furtado, A. J. Ferreira, Humidity sensing properties of a thick-film titania prepared by a slow spinning process, *Sensors and Actuators B.*, **101**, 183–190 (2004).
- [10] Hamid Farahani, Rahman Wagiran, and Mohd Nizar Hamidon, Humidity Sensors Principle, Mechanism, and Fabrication Technologies: A Comprehensive Review, *Sensors.*, **14**, 7881–7939 (2014).